

Research article

Photocatalytic Activity of $\text{LaTi}_{1-x}\text{Fe}_x\text{O}_3$ Perovskite-Type Oxides Under UV and Visible Light

Maria João Nunes^{1*}, André Rodrigues², Paulo Fiadeiro³, Ana Lopes¹, Maria José Pacheco¹, and Lurdes Ciríaco¹

¹FibEnTech-UBI and Department of Chemistry, Universidade da Beira Interior, Rua Marquês d'Ávila e Bolama, 6201-001, Covilhã, Portugal

²Department of Chemistry, Universidade da Beira Interior, Rua Marquês d'Ávila e Bolama, 6201-001, Covilhã, Portugal

³FibEnTech-UBI and Department of Physics, Universidade da Beira Interior, Rua Marquês d'Ávila e Bolama, 6201-001, Covilhã, Portugal

Abstract.

$\text{LaTi}_{1-x}\text{Fe}_x\text{O}_3$ ($x = 0, 0.2, 0.4, 0.6, 0.8$ and 1) perovskite-type oxide samples were synthesized by the solid state reaction method and characterized, and their photocatalytic activity was tested in the degradation of Acid Orange 7 under ultraviolet and visible light. The oxides were successfully synthesized and the XRD results showed a phase change from monoclinic to orthorhombic, with an increase in Fe content (x), with $\text{LaTi}_{0.8}\text{Fe}_{0.2}\text{O}_3$ and $\text{LaTi}_{0.6}\text{Fe}_{0.4}\text{O}_3$ samples presenting both phases. All samples presented low photocatalytic activity under visible light radiation, with a maximum Abs_{484nm} removal of 2.9% for LaFeO_3 after one hour. The best results were obtained under ultraviolet radiation, for all samples, with the best photocatalytic activity exhibited by the $\text{La}_2\text{Ti}_2\text{O}_7$ perovskite, with 44.6% Abs_{484nm} removal after one hour.

Keywords: perovskites, $\text{LaTi}_{1-x}\text{Fe}_x\text{O}_3$, photocatalysis, Acid Orange 7

1. Introduction

Perovskite-type oxides belong to a family of ceramic compounds with a general formula ABO_3 , where A and B are metallic inorganic cations, with $r_A > r_B$ [1,2]. They can occur in many structures, from triclinic to cubic, and are well-known for their versatile and flexible structure, capable of accommodating many cationic combinations without collapsing. This characteristic results in a large variety of properties and applications, such as photocatalysts in the degradation of organic pollutants [3]. The partial substitution of the metallic cations in the LaFeO_3 structure, with other elements, was found to improve its photocatalytic activity [4,5]. Hou et al [4] tested the influence of the partial substitution of La with Li, on the photocatalytic activity degradation of Methyl Blue under UV-Vis radiation. The substitution was found to increase the degradation rate of the dye, with

Corresponding Author: Maria João Nunes; email: maria.nunes@ubi.pt

Published 10 August 2022

Publishing services provided by Knowledge E

© Maria João Nunes et al. This article is distributed under the terms of the Creative Commons Attribution License, which permits unrestricted use and redistribution provided that the original author and source are credited.

Selection and Peer-review under the responsibility of the FibEnTech21 Conference Committee.

 OPEN ACCESS

an optimum amount of Li of $\text{La}_{0.97}\text{Li}_{0.03}\text{FeO}_3$. Similarly, the presence of Ti, in the double-perovskite $\text{La}_2\text{FeTiO}_6$ was assumed to be responsible for the higher p-chlorophenol degradation under visible light, when compared with the results obtained with LaFeO_3 [5]. The aim of this work was to synthesize $\text{LaTi}_{1-x}\text{Fe}_x\text{O}_3$ perovskite-type oxides and test their photocatalytic activity in the degradation of the dye Acid Orange 7 (AO7), under UV and visible light.

2. Material and methods

$\text{LaTi}_{1-x}\text{Fe}_x\text{O}_3$ ($x = 0, 0.2, 0.4, 0.6, 0.8$ and 1) sample powders were synthesized by solid-state reaction. Stoichiometric amounts of La_2O_3 (Acros Organics, 99.9 %), TiO_2 (Aldrich, 99.5 %) and Fe_2O_3 (Merck, 99 %) were mechanically grinded in an agate mortar for 30 min, and heated at 900 °C, for 24 h. Followed by intermediate regrinding and another heating procedure at 1200 °C, for 24 h. All heating procedures were performed in a tubular furnace (Carbolite, model STF) with a Carbolite 3216 temperature controller. All powder samples were structurally characterized by X-ray diffraction (XRD), on a Rigaku, model DMAX II/C with automatic data acquisition (APD Philips v3.5B), equipped with a monochromatized $\text{Cu } k_\alpha$ radiation ($\lambda = 0.15406$ nm), operating at 40 mA and 30 kV. The recording conditions were 2θ between 10 and 90° at a scanning rate of 1.2°/min. The morphological characterization was performed by scanning electron microscopy (SEM), using a Hitachi S2700, operating at 20 keV. Diffuse reflectance spectra (DRS) were measured with a SPEC STD spectrometer (Sarspec), configured with a 25 μm slit, light source, reflectance probe, and reflectance standard, operating in the Ultraviolet/Visible range using a Deuterium Tungsten High Power. The band gap energies (E_g) were calculated from the diffuse reflectance values through the Kubelka-Munk function.

The powders photocatalytic activity was tested under UV and visible light, on the degradation of 10 mg L^{-1} aqueous solutions of AO7 dye (Sigma, 85 %), with radiation provided by a 7 W TUV PL-S lamp (Phillips), emitting at 254 nm, and a 300 W Ultra-Vitalux lamp (Osram), respectively. The 300 W lamp spectrum is shown in Fig.1. The AO7 dye solution volume used was of 10 mL and 160 mL for the photocatalytic assays performed under visible and UV light, respectively. The photocatalytic assays were performed with 0.5 g L^{-1} photocatalyst powder suspensions during 1 h. Prior to both radiation type assays, all suspensions were sonicated for 15 min and stirred, in the dark, for 45 min, to achieve the adsorption-desorption equilibrium between the photocatalyst's surface and AO7 molecules. The dye concentration was monitored by UV-visible absorption spectrophotometry (Shimadzu UV-1800).

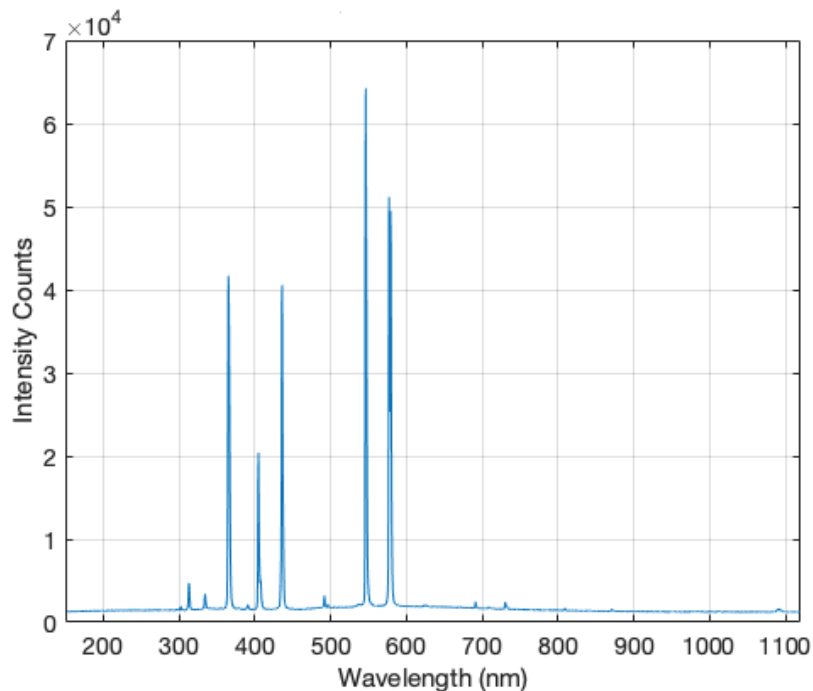


Figure 1: Emission spectrum of the 300 W Ultra-Vitalux UV-visible lamp.

3. Results and discussion

The XRD patterns for all synthesized powders are presented in Fig. 2. The diffractogram corresponding to the $x = 0$ exhibited a well crystallized phase belonging to the $\text{La}_2\text{Ti}_2\text{O}_7$ monoclinic structure, $P21/*$ space group (ICDD file PDF#28-0517). For the $x = 1$ oxide a single well-crystallized phase belonging to the LaFeO_3 orthorhombic structure, $Pbnm$ space group (ICDD file PDF#74-2203) was obtained. With the increase of Fe content (x) a phase change is observed, from a monoclinic to an orthorhombic symmetry, as it can be observed in Fig. 2, through the change of peaks intensity and position. For some samples, such as $x = 0.2$ and 0.4 , both phases were present, but no extra phases were identified.

The morphological characterization results, done by SEM, are in Fig. 3. In these, it is possible to observe a heterogeneous morphology, with the occurrence of different sizes and shapes throughout all samples, with a tendency to agglomerate. It is also evident that the samples corresponding to $\text{La}_2\text{Ti}_2\text{O}_7$ and LaFeO_3 exhibit a bigger average grain size.

The E_g values were obtained through the application of the Kubelka-Munk function on the diffuse reflectance values. This procedure is represented in Fig. 4, with the extrapolation of the linear region of the $(F_{KM} / hv)^2$ vs. hv plot to the abscissa axis for the

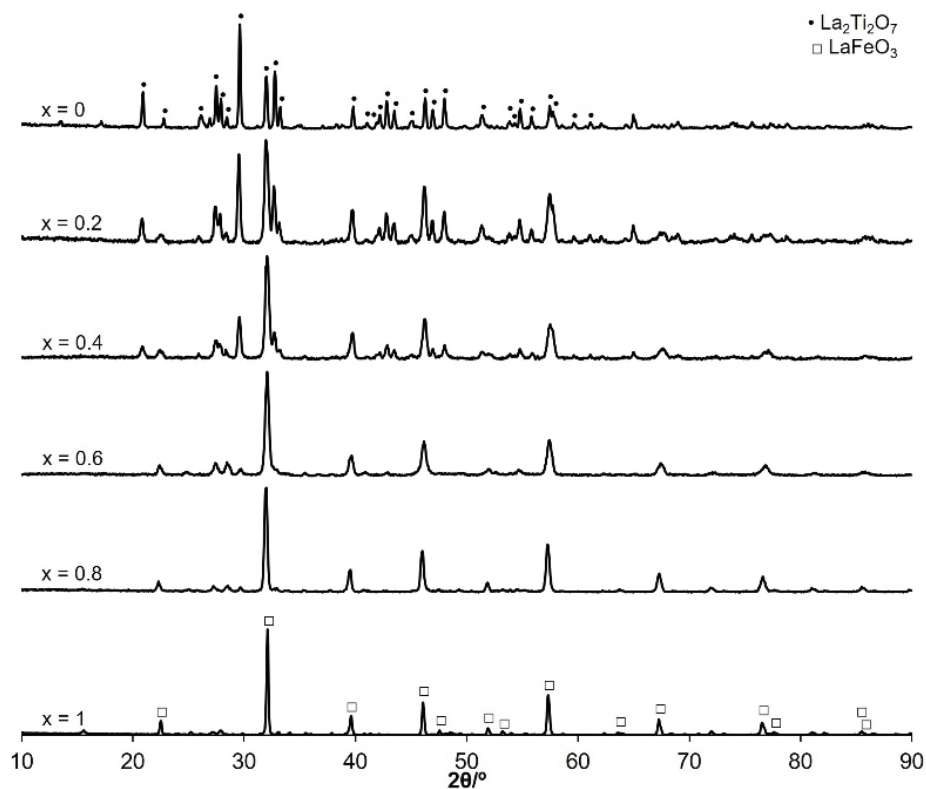


Figure 2: XRD patterns for the $\text{LaTi}_{1-x}\text{Fe}_x\text{O}_3$ oxides.

$\text{La}_2\text{Ti}_2\text{O}_7$ sample, obtaining the E_g value of 3.97 eV. The same procedure was applied for all samples, and all E_g values were obtained (Table 1). For the $\text{LaTi}_{0.8}\text{Fe}_{0.2}\text{O}_3$ and $\text{LaTi}_{0.6}\text{Fe}_{0.4}\text{O}_3$ samples two E_g values were obtained, this could be associated with the presence of two phases in both samples, one predominant, belonging to the monoclinic phase of the $\text{La}_2\text{Ti}_2\text{O}_7$, and one secondary, belonging to the orthorhombic phase of the LaFeO_3 . For the rest of the samples, the E_g values decrease with the increase in Fe content. Regarding the color of the obtained powders, Table 1, the introduction of iron in the perovskite structure results in an orange-like coloration, that gets darker with the increase in Fe content.

The results from the photocatalytic degradation of AO7, under UV and visible light, are presented in Fig. 5. These results show that all synthesized samples do not exhibit favorable photocatalytic activity under visible light, with the best results obtained by the LaFeO_3 ($x = 1$) sample, with an $\text{Abs}_{484\text{nm}}$ removal of 3%, after 1h. These results are in accordance with the high E_g values calculated, for most samples, with the best photocatalytic activity obtained for the oxide with the lowest E_g value. Regarding the results obtained under UV light irradiation, an improvement was observed for all samples, with $\text{Abs}_{484\text{nm}}$ removals from 8% to 45%, the latter obtained by the $\text{La}_2\text{Ti}_2\text{O}_7$ ($x = 0$) perovskite. Further increase in assay time (data not shown) resulted in an

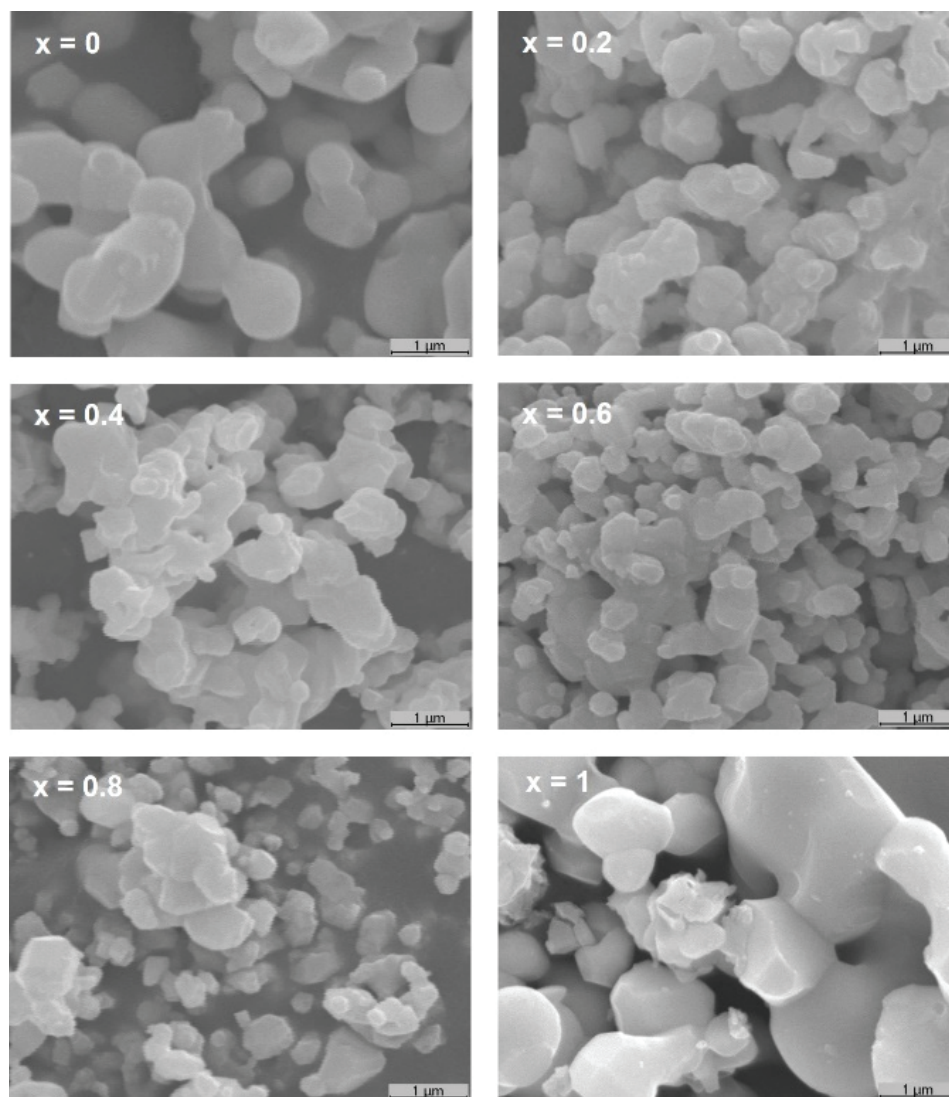


Figure 3: SEM micrographs of all powder samples ($\times 20000$).

Abs_{484nm} removal of 71.1% after 2 h, indicating that, if enough time is employed, complete decolorization, of the AO7 dye solution, could be achieved.

4. Conclusions

All powder samples were successfully synthesized and displayed a phase change with the increase in Fe content, from monoclinic, at $x = 0$, to orthorhombic at $x = 1$. All partially substituted perovskite oxides exhibited smaller average grain size. With the increase in Fe content the E_g decreased, from 3.97 to 2.20 eV and the powders color darkened. All samples exhibited better photocatalytic activity under UV light, with an Abs_{484nm} removal of 47% achieved by the $La_2Ti_2O_7$ sample, after 1 h.

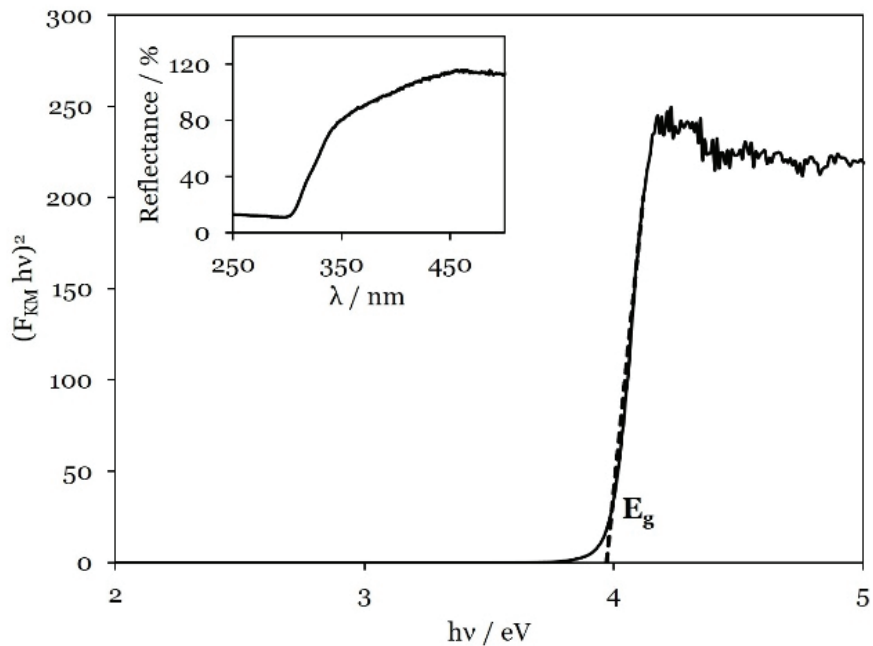


Figure 4: UV-Vis diffuse reflectance spectrum for the La₂Ti₂O₇ oxide. Inset – band gap energy determination.

TABLE 1: E_g values and color of the LaTi_{1-x}Fe_xO₃ oxides.

x	E _g / eV	Color
0	3.97	
0.2	3.42; 3.90	
0.4	3.31; 3.72	
0.6	2.65	
0.8	2.50	
1	2.20	

Acknowledgements

The authors acknowledge the financial support from Fundação para a Ciência e a Tecnologia, FCT, for the project UIDB/00195/2020 of the FibEnTech-UBI Research Unit and for the PhD grant awarded to Maria João Nunes (SFRH/BD/132436/2017 and COVID/BD/151965/2021).

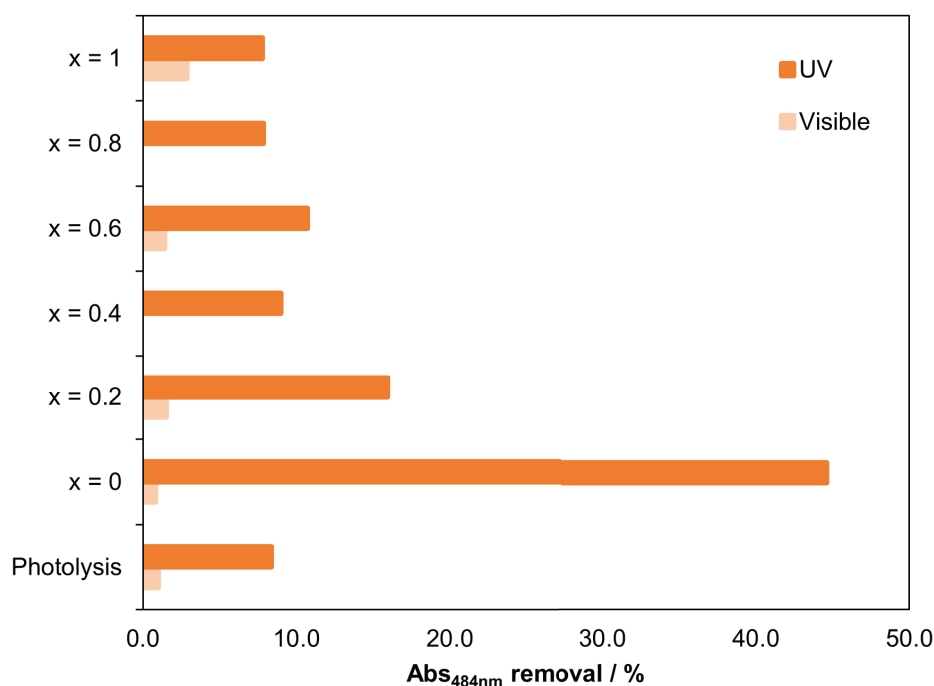


Figure 5: Absorbance removal of the AO7 solutions ($C_i = 10 \text{ mg L}^{-1}$) obtained with the photocatalyst powder suspensions ($C = 0.5 \text{ g L}^{-1}$) under UV and visible light, after 1 h.

References

- [1] Yang Y, Sun Y, Jiang Y. Structure and photocatalytic property of perovskite and perovskite-related compounds. *Materials Chemistry and Physics*. 2006;96(2-3):234-239. <https://doi.org/10.1016/j.matchemphys.2005.07.007>
- [2] Zhu J, Li H, Zhong L, Xiao P, Xu X, Yang X, Zhao Z, Li J. Perovskite oxides: Preparation, characterizations, and applications in heterogeneous catalysis. *ACS Catalysis*. 2014;4(9):2917-2940. <https://doi.org/10.1021/cs500606g>
- [3] Wang W, Tadé MO, Shao Z. Research progress of perovskite materials in photocatalysis- and photovoltaics-related energy conversion and environmental treatment. *Chemical Society Reviews*. 2004;44:5371-5408. <https://doi.org/10.1039/c5cs00113g>
- [4] Hou L, Sun G, Liu K, Li Y, Gao F. Preparation, characterization and investigation of catalytic activity of Li-doped LaFeO_3 . *Journal of Sol-Gel Science and Technology*. 2006;40:9-14. <https://doi.org/10.1007/s10971-006-8368-9>
- [5] Hu R, Li C, Wang X, Sun Y, Jia H, Su H, Zhang Y. Photocatalytic activities of LaFeO_3 and $\text{La}_2\text{FeTiO}_6$ in p-chlorophenol degradation under visible light. *Catalysis Communications*. 2012;29:35-39. <https://doi.org/10.1016/j.catcom.2012.09.012>